On Iterative Detection, Demodulation and Decoding for OFDM-CDM

Armin Dammann[1], Serkan Ayaz[2], Stephan Sand[1], Ronald Raulefs[1]

[1]Institute of Communications and Navigation, German Aerospace Center (DLR), Oberpfaffenhofen, D-82234 Wessling, Germany, Email: {Armin.Dammann, Stephan.Sand, Ronald.Raulefs}@DLR.de

[2]Chair of Mobile Communications, University of Erlangen-Nürnberg, Cauerstrasse 7, D-91058 Erlangen, Germany, Email: sayazim@yahoo.com

Abstract

In this paper, we address iterative receiver processing for *OFDM code division multiplexing (OFDM-CDM)*. The receiver algorithm we focus on is soft parallel interference cancellation in combination with a-priori demodulation. We investigate the convergence behavior of OFDM-CDM as a serial code concatenation, consisting of CDM as inner code and rate-1/2 convolutional codes as outer codes, by means of EXIT chart analysis. The EXIT charts will induce further adaptive modifications for iterative receivers in order to improve the bit error performance. As we will see, performance improvements can be mainly achieved at low signal-to-noise ratios resp. for medium bit error ranges.

1 Introduction

OFDM-CDM and in particular its multiple access variant *multicarrier code division multiple access (MC-CDMA)* are candidate techniques for a 4^{th} generation mobile radio system (4G). Both schemes use typically orthogonal *Walsh-Hadamard (WH)* spreading sequences for their CDM resp. CDMA parts. One focus of ongoing research in OFDM-CDM are advanced receiver algorithms with the cost of an increased computational complexity. Optimum detection/decoding of the entire signal, however, is far to complex for the proposed 4G air interface designs. Iterative detection and decoding algorithms are known to be good suboptimum alternatives. *Soft parallel intererence cancellation (S-PIC)* is one representative [1] of iterative schemes, which is proposed for receivers of OFDM-CDM based systems. For the analysis of the convergence behavior of such concatenated coding schemes with iterative receiver structures, *extrinsic information transfer (EXIT)* charts have become a popular tool [2].

Throughout this paper, we focus on iterative receivers for OFDM-CDM based on the S-PIC receiver principle. Compared to [1] and [3], we additionally include demodulation with a-priori information and use extrinsic rather than a-posteriori information, provided by the outer channel decoder, as a-priori input for the S-PIC. Based on the analysis of the EXIT charts of the OFDM-CDM systems under investigation, we propose approaches for improving the system performance, which are mainly based on adaptive detection and hybrid usage of modulation. Both modifications affect the CDM resp. S-PIC part of the receiver.

In Section 2, we describe the transmitter and receiver structures, we focus on throughout this paper. In Section 3, the principles of adaptive detection and hybrid modulation are introduced together with simulation results in terms of EXIT charts and bit error rate investigations.

2 System Description

The System, we focus on, is a coded OFDM-CDM system in general. In our approach, we use orthogonal *Walsh-Hadamard (WH)* spreading, where all the L available spreading sequences are assigned to one user [3]. Hence, we consider WH-spreading as inner code of a serial concatenated coding scheme rather than as a multiple access component as is typically done in *multi-carrier code division multiple access (MC-CDMA)*. The user separation, i.e. the multiple access, in OFDM-CDM is applied by either FDMA, TDMA or a combination of both. For the channel, we consider an uncorrelated Rayleigh fading channel in frequency domain, i.e. fading is flat per subcarrier with fading coefficients being independently and identically distributed complex valued Gaussian random variables. With this assumption and the respective simulation implementation in frequency domain, we implicitly neglect both *inter-symbol interference (ISI)* and *inter-carrier interference (ICI)*.

2.1 Transmitter

The Transmitter is shown in Fig. 1. We exemplarily consider one user, denoted as *user 1*. The information bits of that user are encoded using rate-1/2 convolutional codes with different constraint lengths. The codebits are then interleaved by a random interleaver and mapped to complex valued data symbols out of a M-QAM modulation alphabet. For our investigations, we use different mappings

$$S: \ \mathrm{GF}(2)^m \rightarrow \mathcal{S} \tag{1}$$

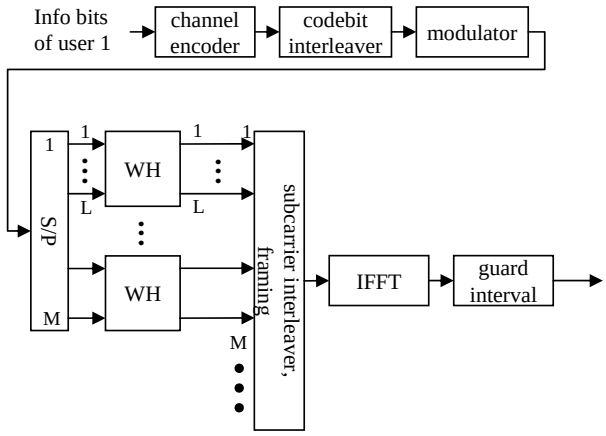

Fig. 1. OFDM-CDM transmitter

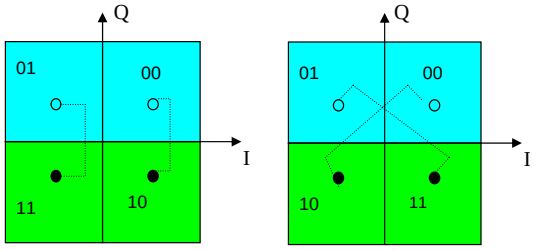

(a) Gray (b) Anti-Gray

Fig. 2. 4-QAM Mappings

as shown in Figs. 2 and 3 as well as in [4] and [5]. Function $S(\underline{c})$ is a one-to-one assignment of binary vectors $\underline{c} \in \mathrm{GF}(2)^m$ to complex valued symbols $s = S(\underline{c}) \in \mathcal{S}$, where the cardinality of $\mathcal{S}$ is $|\mathcal{S}| = 2^m$.

The mappings severely influence the ability of exploiting a-priori information at the demodulator at the receiver [4], [5]. Differently colored areas show the decision regions for the first bit exemplarily. The dotted brackets show subsets of the constellations, where the last $m-1$ bits are equal, i.e. these subsets remain for demodulation of the first bit if the last $m-1$ bits would perfectly be known. It is typical for Gray mappings, that the minimum Euclidean distance between constellation points of the subsets does not increase, even if a-priori knowledge is available.

After modulation, M complex valued user data symbols are serial-to-parallel converted and grouped into

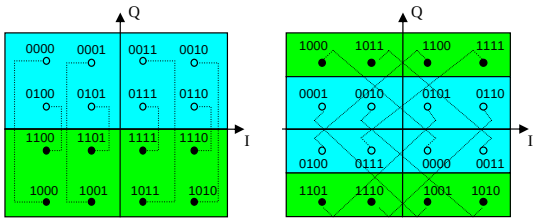

(a) Gray (b) Modified Set Partitioning (MSP)

Fig. 3. 16-QAM Mappings

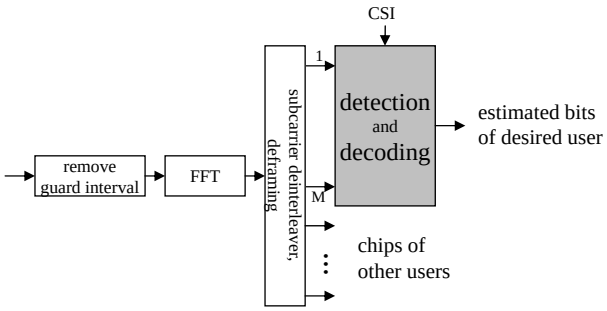

Fig. 4. Generic OFDM-CDM receiver structure

M/L data symbol vectors $\underline{S}^i = [S_1^i, \ldots, S_L^i]$, $i = 1, \ldots, M/L$ of length L. Multiplying $\underline{S}^i$ with an $L \times L$ WH spreading matrix, which is recursively defined by

$$\mathbf{W}_{2\ell} = \begin{pmatrix} \mathbf{W}_\ell & \mathbf{W}_\ell \\ \mathbf{W}_\ell & -\mathbf{W}_\ell \end{pmatrix}, \quad \mathbf{W}_1 = (1), \qquad (2)$$

yields the chips $\underline{b}^i = \underline{S}^i \cdot \mathbf{W}_L$. Here, L is a power of 2 and M is an integer multiple of the spreading factor L. The N_c data symbols are randomly interleaved and mapped to the N_c used subcarriers of an OFDM symbol. An *inverse fast Fourier transform (IFFT)* of length $N_\mathrm{FFT} \geq N_\mathrm{c}$ transforms the data symbols in frequency domain into time domain. Possibly remaining $N_\mathrm{FFT} - N_\mathrm{c}$ subcarriers are zero padded. To prevent ISI caused by multipath propagation, a guard interval (cyclic prefix) is inserted in time domain before transmission.

2.2 Receiver

Fig. 4 shows the generic receiver structure. After removal of the guard interval, the OFDM symbol is transformed into frequency domain by an FFT. The subcarriers are deinterleaved and the M user data symbols per OFDM symbol are extracted and fed into a detection and decoding entity. For OFDM-CDM ($L > 1$), we use *soft parallel interference cancellation (S-PIC)* as described in Section 2.2.1. For $L = 1$, our system degrades to a simple coded OFDM system. The detection and decoding is introduced in the following subsection. Additionally, we assume perfect knowledge of *channel state information (CSI)*.

2.2.1 Soft Parallel Interference Cancellation

For OFDM-CDM with $L > 1$ we use an iterative *soft parallel interference cancellation (S-PIC)* algorithm. In [1] and [3] this algorithm was proposed for MC-CDMA resp. OFDM-CDM. Fig. 5 shows the detection and decoding part of a soft parallel interference canceller, which additionally exploits a-priori information at the demodulator as shown in 2.2.2. The basic idea of S-PIC is to replace the hard decision remodulator in the signal reconstruction parts of a conventional interference canceller by a soft symbol mapper. Whereas hard decision remodulation provides $\hat{S} = \arg\max_{S(\underline{c})} P(S(\underline{c}))$, i.e. the most probable symbol, soft symbol mapping

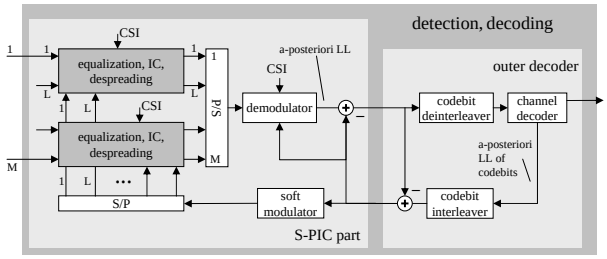

Fig. 5. Detection and decoding part of a soft parallel interference canceller

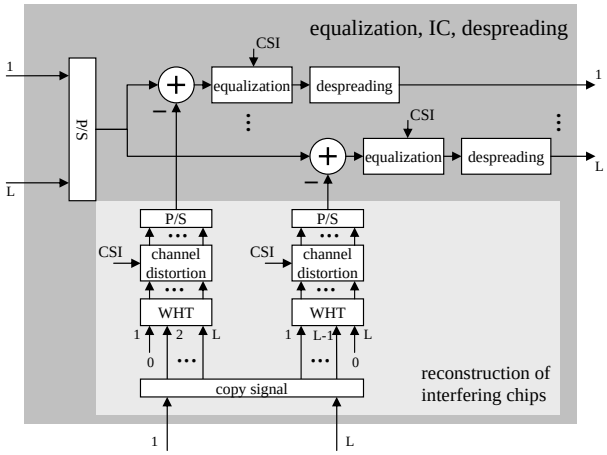

Fig. 6. Equalization, interference cancellation and despreading part of an S-PIC

calculates

$$\bar{S} = E\{S(\underline{c})\} = \sum_{\underline{c} \in \mathrm{GF}(s)^m} S(\underline{c}) \cdot P(S(\underline{c})) \qquad (3)$$

and use these mean values for the signal reconstruction section of the S-PIC. For the calculation of the soft symbol, we need the probability of each symbol, which can be calculated from *log-likelihood ratios (LLRs)* provided to the soft symbol mapper by the outer channel decoder:

$$P(S(\underline{c})) = \prod_{j=1}^{m} \frac{e^{-c_j \cdot L^{\mathrm{a}}(c_j)}}{1 + e^{-L^{\mathrm{a}}(c_j)}} \qquad (4)$$

$S(\underline{c})$ describes the used mapping and $\underline{L}^{\mathrm{a}}(\underline{c}) = [L^{\mathrm{a}}(c_1), \ldots, L^{\mathrm{a}}(c_m)]$ is a vector of LLRs assigned to codebits $\underline{c} = [c_1, \ldots, c_m]$. In Fig. 5 equalization, interference cancellation and despreading is shown as a 'gray-box'. This gray-box is shown in detail in Fig. 6. In principle, the S-PIC consists of L parallel *single user detection (SUD)* branches (One for each of the L spreading sequences). In each of these branches, the signal components of the respective other spreading sequences are subtracted based on the soft remodulated data symbols and the CSI. Before despreading in the SUD branches, each chip is equalized by multiplication of a complex valued scalar equalizer coefficient. In our investigations, we focus on *minimum mean square error (MMSE)* equalization. The equalizer coefficients for that are calculated as

$$G^{\mathrm{MMSE}} = \frac{H^*}{|H|^2 + \frac{\sigma_{\mathrm{N}}^2}{\lambda}}, \qquad (5)$$

where $(\cdot)^*$ denotes the complex conjugate operation. σ_{N}^2 is the variance of the complex *additive white Gaussian noise (AWGN)*, which corrupts each subcarrier. Parameter $\lambda = \frac{K}{L}$ is dependent on the number of used spreading codes K and the spreading code length L, i.e., λ indicates the signal power for each chip. For MC-CDMA, K denotes the number of users in the system. In OFDM-CDM, however, $\lambda = 1$ at the beginning, since all available spreading codes are used in the CDM part. In further S-PIC iterations, the interfering spreading codes' signal parts are cancelled in each SUD branch. Therefore, parameter λ can somehow be optimized dependent on the amount of a-priori information provided by the outer channel decoder. The range for optimization varies from $\lambda = \frac{1}{L}$ if interference can be cancelled out perfectly up to $\lambda = 1$ if no a-priori information is available at all. Note that if λ decreases, G^{MMSE} approaches — except for a constant — the equalizer coefficient for *maximum ratio combining (MRC)*, $G^{\mathrm{MRC}} = H^*$. MRC, however, is the optimum with respect to the signal-to-noise ratio of each chip if only one spreading code is used, i.e., if we can assume perfect interference cancellation.

2.2.2 Demodulation

For the demodulator, we assume, that the complex valued data at the input can be expressed as

$$R = S \cdot H + N, \qquad (6)$$

where S and H denote the sent symbol resp. a fading coefficient. N is AWGN with zero mean and variance $\sigma^2/2$ in both real and imaginary part. For notational convenience, we neglect any time resp. frequency index. In OFDM-CDM, the fading coefficient H for demodulation can be calculated from the channel (subcarrier) fading coefficients (CSI), $H_\ell,\ \ell = 1, \ldots, L$, which influence the chips to be despread, and the associated equalizer coefficients G_ℓ by

$$H = \frac{1}{L} \sum_{\ell=1}^{L} H_\ell \cdot G_\ell. \qquad (7)$$

We use MMSE equalization as defined in (5). The variance of the noise term N is

$$\sigma^2 = \underbrace{\frac{(K-1)}{L} \cdot \left(\frac{1}{L} \sum_{\ell=1}^{L} |H_\ell \cdot G_\ell|^2 + \left| \frac{1}{L} \sum_{\ell=1}^{L} H_\ell \cdot G_\ell \right|^2 \right)}_{\sigma_{\mathrm{SI}}^2} + \underbrace{\frac{\sigma_{\mathrm{N}}^2}{L} \cdot \sum_{\ell=1}^{L} |G_\ell|^2}_{\sigma_{\mathrm{Gauss}}^2}, \qquad (8)$$

which consists of a Gaussian noise part and a self interference part [3]. Eq. (8) is originally derived for MC-CDMA, where K denotes the number of active

users, i.e. the number of used spreading codes, and is therefore as well related to the optimization parameter λ as introduced in Section 2.2.1. The a-posteriori LLRs of bits $i, i = 1, \ldots, m$ are calculated as

$$L(c_i) = \log \frac{\sum\limits_{\substack{\underline{c} \in \mathrm{GF}(2)^m \\ c_i = 0}} P(R|S(\underline{c})) \cdot \prod\limits_{j=1}^{m} e^{-c_j \cdot L^{\mathrm{a}}(c_j)}}{\sum\limits_{\substack{\underline{c} \in \mathrm{GF}(2)^m \\ c_i = 1}} P(R|S(\underline{c})) \cdot \prod\limits_{j=1}^{m} e^{-c_j \cdot L^{\mathrm{a}}(c_j)}}, \tag{9}$$

where again $\underline{L}^{\mathrm{a}}(\underline{c}) = [L^{\mathrm{a}}(c_1), \ldots, L^{\mathrm{a}}(c_m)]$ is a vector of LLRs assigned to codebits $\underline{c} = [c_1, \ldots, c_m]$. These values are provided by the (outer) channel decoder in terms of extrinsic LLRs. In (9), $\prod_{j=1}^{m} e^{-c_j \cdot L^{\mathrm{a}}(c_j)}$ is proportional to the (a-priori) symbol probability $P(S(\underline{c}))$, calculated according to (4). Since we assume AWGN in (6), the conditional probability $P(R|S(\underline{c}))$ follows from a complex valued Gaussian distribution, i.e.

$$P(R|S(\underline{c})) = \frac{1}{\pi \cdot \sigma^2} \cdot e^{-\frac{|R - S(\underline{c}) \cdot H|^2}{\sigma^2}}. \tag{10}$$

The extrinsic LLRs

$$L^{\mathrm{e}}(c_j) = L(c_j) - L^{\mathrm{a}}(c_j), \quad j = 1, \ldots, m \tag{11}$$

are provided to the channel decoder for soft-in/soft-out decoding. Subsequently, we use convolutional codes, decoded by the Log-MAP algorithm [6], [7].

3 Adaptive Detection and Hybrid Modulation

In this section, we introduce ideas, how to adapt detection and modulation for different amounts of a-priori information. For our investigations, we use EXIT chart analysis to quantify 'a-priori information' in terms of mutual information [2]. Additionally, we investigate bit error performances by simulations.

3.1 Adaptive Detection in Iterative OFDM-CDM Receivers

As already mentioned in Section 2.2.1, parameter λ can be optimized, dependent on the available a-priori information, provided by the outer channel decoder. In Fig. 7, we first show the EXIT characteristics of a S-PIC as shown in Fig. 5 with $\lambda = 8/8$, $L = 8$, 4-QAM (Anti-Gray) for $E_{\mathrm{b}}/N_0 = 3\mathrm{dB}$[1] and a (133,171) convolutional code with Log-MAP decoding. Note, that the EXIT characteristic of the channel decoder does not depend on the signal-to-noise ratio (E_{b}/N_0). For the parameters, mentioned above, the *tunnel*, which the area between detector and decoder EXIT characteristic of the EXIT chart, provides a connection from the EXIT chart origin to a mutual information value close to 1 at the decoder output. Therefore, it is possible for the iterative detection/decoding process to *converge*

[1]The definition of E_{b}/N_0 takes into account the code rate R of the outer channel code as well as the number of bits m per data symbol.

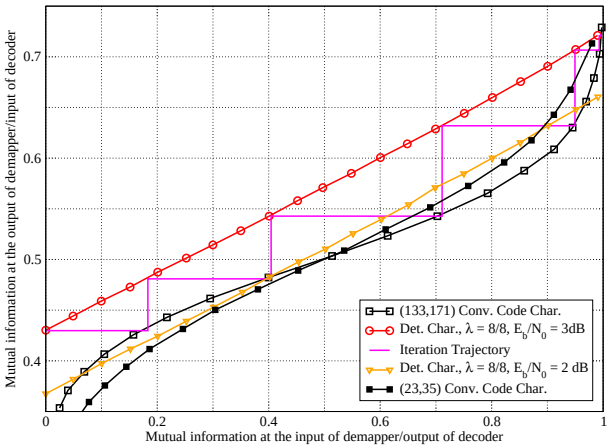

Fig. 7. EXIT characteristics of S-PIC and conv. codes for $\lambda = 8/8$, $L = 8$, 4-QAM (Anti-Gray), uncorrelated Rayleigh fading channel

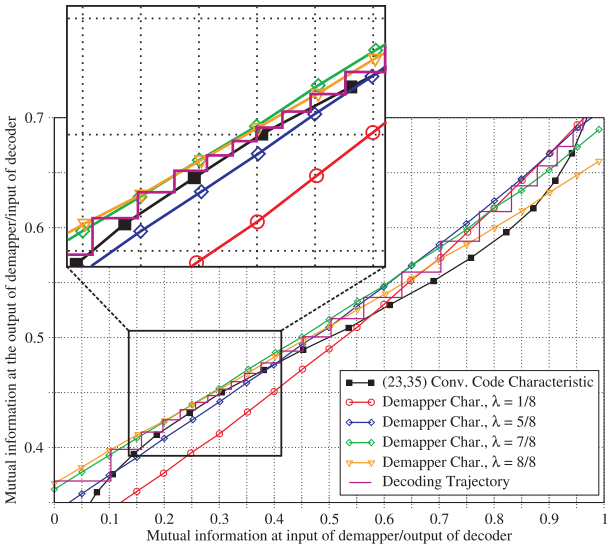

Fig. 8. EXIT characteristic of S-PIC for different values of λ, $L = 8$, 4-QAM (Anti-Gray), uncorrelated Rayleigh fading channel, $E_{\mathrm{b}}/N_0 = 2\mathrm{dB}$

against a detector output mutual information value of 1. The convergence behavior is shown by the decoding trajectory in Fig. 7. However, if we decrease the SNR to $E_{\mathrm{b}}/N_0 = 2\mathrm{dB}$, the tunnel vanishes. If we use a (23,35) convolutional code, which has a lower constraint length, we again observe a tunnel. This tunnel is very narrow and the EXIT characteristics of S-PIC and decoder intersect at about 0.89 for the mutual information at the output of the decoder. To increase this intersection point, i.e. to decrease the bit error rate, we decrease λ with an increasing number of iterations. Fig. 8 shows the EXIT characteristics of the S-PIC part for $E_{\mathrm{b}}/N_0 = 2\mathrm{dB}$ and different values of λ. This adaptation does not widen the tunnel significantly. However, we increased the intersection point with the decoder characteristic, which results in a decreased bit error rate. Starting with $\lambda = 8/8$, we switch to $\lambda = 7/8,\ 5/8,\ 1/8$ after 4, 15 and 20 iterations respectively. Fig. 9 shows the bit error rates vs. E_{b}/N_0. For comparison, we show the BERs for *single user detection (SUD)*, which is equal

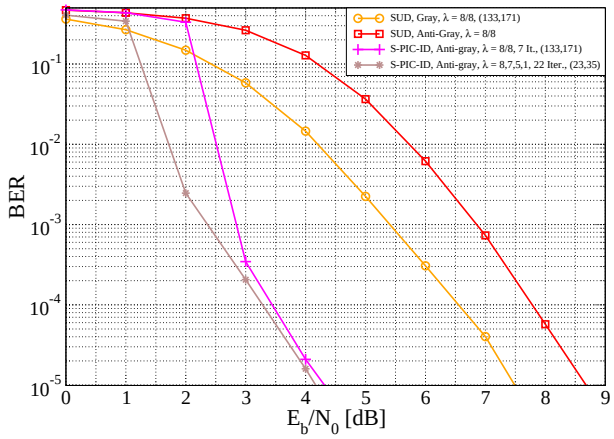

Fig. 9. BER vs. E_b/N_0 for S-PIC and different values of λ, $L = 8$, 4-QAM (Anti-Gray), uncorrelated Rayleigh fading channel

to the performance of an S-PIC after the 0^{th} iteration. It can be seen, that for non-iterative receivers, 4-QAM Gray mapping significantly outperforms 4-QAM Anti-Gray mapping. Since 4-QAM with Anti-Gray mapping is able to exploit a-priori information, we choose this mapping when increasing the number of iterations. It can be seen, that we can improve the BER at lower SNR regions if we use an adaptive S-PIC together with a convolutional code with lower constraint length. The results, shown above indicate system performance improvements by using adaptive S-PIC. For the optimum case, the EXIT characteristic of the S-PIC has to be maximized with respect to λ and the mutual input information. It is obvious from Fig. 8, that λ depends on the mutual information at the S-PIC input. However, this would require an adequate estimation and tracking of the S-PIC input mutual information. Furthermore, it is not clear, how the performance compares to a robust design, where $\lambda = L/L = 1$ is used for each iteration except for the last one, where $\lambda = 1/L$ could be a proper choice.

3.2 Hybrid Modulation

In [4], [5] and [8] several mappings were proposed, which differ in their EXIT characteristic. Differences are mainly in the steepness, which determine somehow the ability of exploiting a-priori information, and in the offset, which is the mutual information output of the demodulator for zero a-priori information input. It can be observed qualitatively, that the higher the offset, the lower is the steepness of the EXIT characteristic. In order to adjust EXIT characteristics, the idea here is to mix several mappings within a data stream. Fig. 10 exemplarily shows this principle for 16-QAM with Gray- and *modified set partitioning (MSP)* mapping (see Fig. 3), used in a ratio of $\alpha = 1/1$. For our simulations, we use a OFDM-CDM system with S-PIC at the receiver as introduced in the previous section. The spreading factor is $L = 8$. Equalization within the S-PIC is MMSE with $\lambda = 8/8 = 1$, i.e. we do not use adaptive detection. The outer code is a (23,35) rate-1/2 convolutional code.

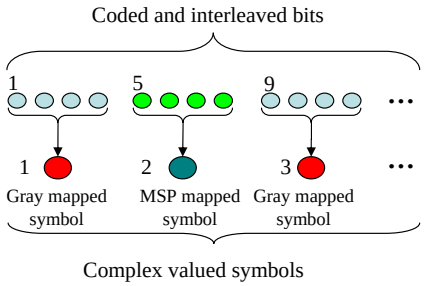

Fig. 10. Principle of hybrid modulation

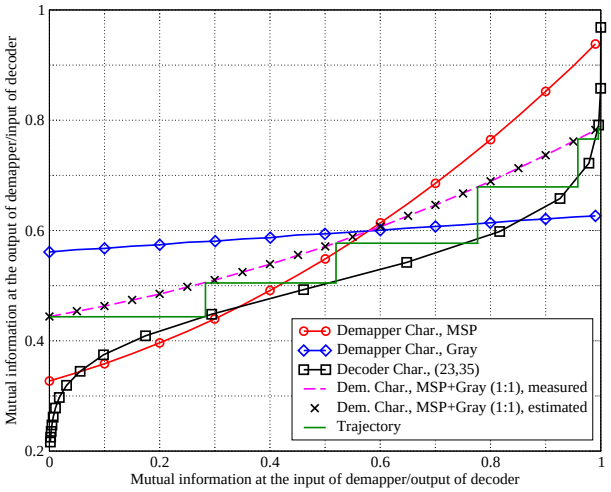

Fig. 11. EXIT characteristics for S-PIC, hybrid modulation using 16-QAM with Gray and MSP mapping, uncorrelated Rayleigh fading channel, $E_\mathrm{b}/N_0 = 7\mathrm{dB}$

Fig. 11 shows the EXIT characteristics of 16-QAM with Gray resp. MSP mapping for $E_\mathrm{b}/N_0 = 7\mathrm{dB}$ as well as the (23,35) convolutional decoder characteristic. It can be seen, that neither Gray nor MSP mapping predicts a reasonable performance. For MSP no tunnel at all can be observed. The first intersection with the decoder characteristic is at a mutual demodulator input information of about 0.05. For Gray mapping, the intersection point is at about 0.85, which still does not promise a low BER, and, since the demodulator characteristic is rather flat, we cannot benefit significantly from increasing the number of iterations. Following the approach of irregular mappings in [9] by using Gray and MSP mapping alternatively as depicted in Fig. 10 yields a demodulator characteristic, which is a weighted average of the component characteristics, i.e. of Gray and MSP mapping in our case. On the one hand, this hybrid characteristic shows a reasonable steepness, so that we can benefit from iterative detection/decoding. On the other hand, the intersection point with the decoder characteristic is at about 0.99, which predicts a low BER. It can further be seen, that the hybrid characteristic can be estimated quite well by averaging the component Gray and MSP characteristics, taking into account the mapping ratio α, which is $\alpha = 1:1 = 1$ in our case. The dashed line shows the measured characteristic, whereas the cross markers are calculated from the component characteristics $T_{\mathrm{Gray}}(x)$

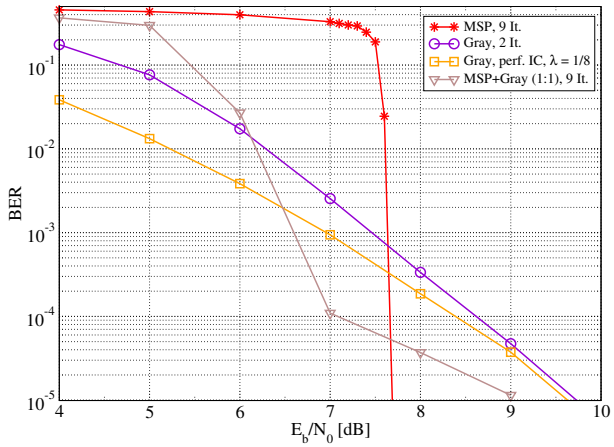

Fig. 12. BER vs. E_b/N_0 for hybrid modulation using 16-QAM with Gray and MSP mapping, uncorrelated Rayleigh fading channel

and $T_\mathrm{MSP}(x)$ by

$$T_\mathrm{Hybrid}(x) = \frac{1}{2}\left(T_\mathrm{Gray}(x) + T_\mathrm{MSP}(x)\right), \qquad (12)$$

as derived in [9], where x is the mutual information at the demodulator input.

Fig. 12 shows the BER performance for hybrid modulation, exemplarily described previously. It can be seen, that hybrid modulation outperforms pure Gray resp. MSP mapping at BER of 10^{-2} down to about 10^{-4}. For Gray mapping, we have chosen 2 iterations, since the system performance cannot be improved significantly by further iterations due to the flat EXIT characteristic of 16-QAM Gray mapping. For comparison, we show the BER performance for 16-QAM Gray mapping with perfect interference cancellation.

4 Summary and Outlook

In this paper, we investigated iterative receiver algorithms for OFDM-CDM. For detection of the CDM part, we used an S-PIC, which exploits a-priori information in both its cancellation part and demodulation part. We have considered channel coding and CDM as serial code concatenation and analyzed its convergence behavior by means of EXIT chart analysis. These analysis induced the idea of adaptive detection and hybrid modulation. The concept of hybrid modulation provides a method for adapting the demodulator characteristic, i.e. to design 'good compromises', where the hybrid characteristic, at least in our simulations, could be estimated by a weighted average of the component characteristics. With these approaches, performance improvements at low to medium SNRs, i.e. medium bit error rates in the range of 10^{-2} down to about 10^{-4} can be achieved, which has exemplarily be shown by simulations.

Since this adaptation mainly relies on the knowledge of the mutual a-priori information content, further investigations on the estimation of that information will be necessary. One further interesting question in this direction is whether the EXIT characteristic intersection points for differently adapted S-PICs (i.e. different parameters λ or different mappings) severely depend on the channel SNR. Furthermore the investigation of the introduced adaptive and hybrid techniques for multipath fading channels is of interest.

The techniques introduced above are approaches for exploiting adaptivity at iterative OFDM-CDM receivers, where we do not use repeated transmissions, e.g. for streaming applications or broadcasting systems. Another degree of freedom for hybrid mapping is provided by systems including an *automatic repeat request (ARQ)* component. For such systems it can be beneficial to start data transmission using Gray mapping due to its high offset and switch to a-priori information exploiting mapping schemes for further retransmissions, where information of previous ARQ transmissions is used as a-priori for the current one. This could promise performance improvements especially in low SNR regions.

Acknowledgement

The authors are very grateful to Prof. Wolfgang Koch, head of the Chair of Mobile Communications at the University of Erlangen-Nürnberg. He supported this work in the framework of the Master Thesis of Serkan Ayaz. This research has been conducted within the NEWCOM Network of Excellence in Wireless Communications funded through the EC 6^{th} Framework Programme.

References

[1] Stefan Kaiser and Joachim Hagenauer. Multi-carrier CDMA with iterative decoding and soft-interference cancellation. In *Proceedings IEEE Global Telecommunications Conference (GLOBECOM 1997), Phoenix, USA*, volume 1, pages 6–10, November 1997.

[2] Stephan ten Brink. Convergence behavior of iteratively decoded parallel concatenated codes. *IEEE Transactions on Communications*, 49(10):1727–1737, October 2001.

[3] Stefan Kaiser. OFDM code division multiplexing in fading channels. *IEEE Transactions on Communications*, 50(8):1266–1273, August 2002.

[4] Aik Chindapol and James A. Ritcey. Design, analysis, and performance evaluation for BICM-ID with square QAM constellations in Rayleigh fading channels. *IEEE Journal on Selected Areas in Communications*, 19(5):944–957, May 2001.

[5] Frank Schreckenbach, Norbert Görtz, Joachim Hagenauer, and Gerhard Bauch. Optimized symbol mappings for bit-interleaved coded modulation with iterative decoding. In *Proceedings IEEE Global Telecommunications Conference (GLOBECOM 2003), San Francisco, CA, USA*, volume 6, pages 3316–3320, December 2003.

[6] L. Bahl, J. Cocke, F. Jelinek, and J. Raviv. Optimal decoding of linear codes for minimizing symbol error rate. *IEEE Transactions on Information Theory*, 20(2):284–287, March 1974.

[7] Patrick Robertson, Emmanuelle Villebrun, and Peter Höher. A comparison of optimal and sub-optimal map decoding algorithms operating in the log domain. In *Proceedings IEEE International Conference on Communications (ICC 1995), Seattle, USA*.

[8] Jun Tan and Gordon L. Stüber. Analysis and design of interleaver mappings for iteratively decoded BICM. In *Proceedings IEEE International Conference on Communications (ICC 2002), New York, USA*, volume 25, pages 1403–1407, April 2002.

[9] Frank Schreckenbach and Gerhard Bauch. Irregular signal constellations, mappings and precoder. In *International Symposium on Information Theory and its Applications (ISITA), Parma, Italy*, October 2004.